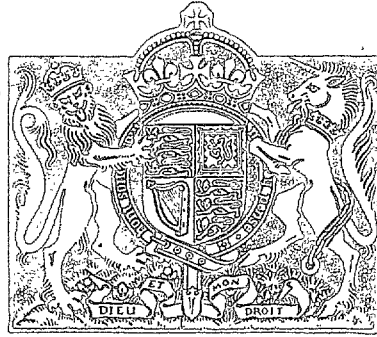


MINISTRY OF SUPPLY
AERONAUTICAL RESEARCH COUNCIL
LIBRARY

N.A.E.
NATIONAL AERONAUTICAL ESTABLISHMENT
LIBRARY

R. & M. No. 2552
(7473)
A.R.C. Technical Report



NATIONAL AERONAUTICAL
ESTABLISHMENT
20 MAY 1952
THE CLYDE BLDG.

MINISTRY OF SUPPLY

AERONAUTICAL RESEARCH COUNCIL
REPORTS AND MEMORANDA

The Prevention of Binary Flutter by Artificial Damping

By

R. A. FRAZER, B.A., D.Sc.
of the Aerodynamics Division, N.P.L.

Crown Copyright Reserved

LONDON: HIS MAJESTY'S STATIONERY OFFICE

1951

PRICE 4s 6d NET

The Prevention of Binary Flutter by Artificial Damping

By

R. A. FRAZER, B.A., D.Sc.,
of the Aerodynamics Division, N.P.L.

Reports and Memoranda No. 2552

16th February, 1944

Summary.—Range of Investigation.—Formulae are obtained which provide an estimate of the amount of artificial control needed to prevent binary flutter. Results are expressed in terms of a 'minimum damping multiplier' R , defined as the ratio of the least direct damping coefficient required for absolute flutter prevention to the 'natural' direct aerodynamic damping coefficient of the control surface concerned. Numerical results are obtained for five different types of aircraft.

Conclusions.—The main conclusions are as follows:—

- (i) R varies with the type of flutter and increases markedly with height.
- (ii) Large values of R are to be expected with high structural density or mass-underbalance of the control surfaces.
- (iii) Maximum height should (in general) be assumed in the estimation of artificial damping.
- (iv) With artificial damping of conventional type servo-operated controls and devices for reduction or cut-out of the damping at low speeds will normally be necessary.
- (v) If artificial damping is applied to a main control surface, mass-balancing of the servo-flap may be necessary.

1. *Introduction and Conclusions.*—The theoretical advantages of heavily damped control surfaces from the standpoint of flutter prevention have long been recognized.* Recently it has been suggested that artificial damping might be preferable to mass-balancing as a means of preventing flutter, since weight might be saved. The purpose of the present paper is to provide simple formulae from which the amount of additional damping required can be estimated.

Attention is restricted to binary flutter, which is referred to as being of Class A or B according to the nature of the dynamical coefficients (*see* Table 1). With Class A two of the aerodynamical stiffness coefficients are zero ($c_1 = c_2 = 0$); whereas with Class B all the aerodynamic stiffnesses are present. The formulae obtained differ for the two classes of flutter. The detailed proofs, which assume simple classical derivative theory and depend on the properties of test conics,† are given in the Appendix. In general, the control surfaces considered are assumed to be mass underbalanced.

The damping values obtained are theoretically sufficient for the absolute prevention of flutter (*i.e.* prevention for all elastic stiffnesses). In practice, increased values should be taken, to allow for uncertain data. For convenience, results are expressed in terms of a minimum *damping multiplier* R , which is defined as the ratio of the least direct damping coefficient required for absolute flutter prevention to the 'natural' direct aerodynamic damping coefficient of the control surface concerned. The value of R varies with the altitude h owing to the increasing influence of the structural inertias with decreasing air density ρ .

* *See*, for example, recommendation (e) of section 9, R. & M. 1155¹. Also Conclusion (d) on p. 1 of R. & M. 1685².

† *See* Chapters III and VIII of R. & M. 1155¹.

In practice, artificial damping proportional to ρ and to airspeed V (and thus providing an increase of damping *coefficient*) is unlikely to be achieved by any simple means. If the device used provides merely *constant* additional damping, the amount of this should be of sufficient magnitude to ensure that at any height h (ft), and for the corresponding true maximum diving speed V_m (ft/sec) flutter is absent. The total effective damping coefficient will then be on the safe side for other flight conditions. Suppose, for example, that the case considered is flexural-aileron flutter, and let the coefficients* be defined as in Table 1(a). Then if R denotes the minimum damping multiplier corresponding to air density ρ , the constant artificial aileron damping to be supplied is given by

$$K = \rho (R - 1) V_m l c_0^3 e_2, \dots \dots \dots (1)$$

where the height should be chosen such that $\rho (R - 1) V_m$ has its greatest value. In this case the effective damping multiplier for any other air density ρ' and for any speed $V' \leq V_m$ will be

$$1 + \frac{\rho V_m (R - 1)}{\rho' V'}$$

which will certainly exceed R' , the minimum multiplier corresponding to air density ρ' . Numerical examples given in sections 2 and 3 indicate that (in general) maximum height should be assumed in the estimation of K . In the absence of definite information the value of V_m is taken to be independent of the height in the examples.

The quantity K in (1) measures the aileron hinge moment (in lb ft) due to artificial damping when the aileron is rotated steadily at a rate of 1 rad/sec.

(a) *Damping Formulae for Class A Flutter.*—This class is represented by standard flexural-aileron flutter and by rudder flutter involving fuselage torsion. The formulae, which involve one or both of the moment-of-inertia coefficients as well as the product-of-inertia coefficient p , differ according to the sign of β (for symbols, see Table 1(a)).

Case (i). *Flexural-Aileron Flutter* ($f_2 > 0, \beta > 0$).

The value of R is here given by the greatest positive root of the equation

$$b_1^2 e_2^2 R^2 - b_1 e_2 (b_2 e_1 + p f_1) R + b_2 f_1 \{p (e_1 + b_2) - d_2 b_1\} = 0 \dots \dots \dots (A_1)$$

Case (ii). *Rudder-torsional Flutter* ($f_2 > 0, \beta < 0$).

For (A₁) substitute

$$\{a_1 e_2 R + b_1 d_2 - p (e_1 + b_2)\} \{b_1 e_2 R - b_2 e_1 - p (e_1 + b_2)\} + (a_1 d_2 - p^2) b_2 f_1 = 0 \dots \dots (A_2)$$

Conditions (A₁) and (A₂) ensure test conic diagrams of the types Figs. 1(c) and 1(b) respectively.

(b) *Damping Formulae for Class B Flutter.*—This class includes most other varieties of flutter (e.g. torsional-aileron, servo-rudder, elevator-fuselage, etc.). The formulae are independent of the moments of inertia.

Let μ_1, μ_2 denote the two roots of the equation

$$\mu^2 - \{e_3 j_2 + 2p (k_2 + f_3)\} \mu + p^2 (k_2 - f_3)^2 + p \beta (j_2 + e_3) = 0 \dots \dots \dots (2)$$

Then if μ_1, μ_2 are real ($\mu_2 > \mu_1$) the multiplier R to be applied to the product $e_2 j_3$ of the two natural direct damping coefficients is given by

$$R = \mu_1 / e_2 j_3 \dots \dots \dots (B_1)$$

If μ_1, μ_2 are unreal, choose

$$R = \beta^2 / 4 e_2 j_3 k_2 f_3 \dots \dots \dots (B_2)$$

* If the coefficients used are not non-dimensional, the formulae should be applied with l and c_0 suppressed.

Conditions (B₁) and (B₂) correspond respectively to test conic diagrams of the types Fig. 2(d), and Fig. 2(b) with T below H_u . With types of flutter other than those considered in this paper the formulae used should be guided by the geometry of the test diagram.

Numerical results for some representative aircraft and for various types of flutter are summarized in Table 2. The following conclusions are indicated by the calculations.

General Conclusions.—(i) The minimum damping multiplier R varies with the type of flutter and increases markedly with height.

(ii) Large values for R are to be expected with high structural density or pronounced mass underbalance of the control surfaces.

(iii) Maximum height should (in general) be assumed in the estimation of the artificial damping K .

(iv) With artificial damping of conventional type, servo-operated controls and devices for reduction or cut-out of the damping at low speeds will normally be necessary.

(v) If artificial damping is applied to a main control surface, mass-balancing of the servo-flap may be unnecessary.

It is considered probable that an aileron which is adequately damped to prevent flexural-aileron and torsional-aileron flutter, will also prove to be adequately damped against ternary flutter and tab-aileron flutter. However, a verification of this conjecture by calculation would be desirable before artificial damping were tried out in practice.

2. *Numerical Examples (Class A Flutter).*—(i) *Flexural-Aileron Flutter (Fighter Aircraft).*—The data are taken from the end of section 2, R. & M. 2551³, and relate to a fighter aircraft (aircraft S of Ref. 5). The dimensions, in feet, for full-scale are

$$\begin{aligned} c_0 \text{ (root-chord of wing)} &= 5.87 \\ s \text{ (span of one wing)} &= 18.5 \\ c_a \text{ (aileron mean chord)} &= 1.38 \\ s_a \text{ (aileron span)} &= 6.85 \\ l = 0.57s &= 10.54 \end{aligned}$$

Aerodynamic Coefficients (non-dimensional, Table 1(a))

$$\begin{aligned} b_1 = 5.78, & & e_1 = 0.298, & & f_1 = 1.39, \\ b_2 = 0.00972, & & e_2 = 0.009225, & & f_2 = 0.0146. \end{aligned}$$

Aerodynamic Inertial Coefficients (non-dimensional)

$$p_0 = 0.0162, \quad d_{20} = 0.00054.$$

Total Inertial Coefficients (Structural plus Aerodynamic)

Altitude (ft)		0	10,000	20,000	30,000	40,000
ρ_0/ρ		1.0	1.35	1.88	2.67	4.06
Fabric aileron covering	$\frac{p}{d_2}$	0.0998 0.00587	0.128 0.00773	0.173 0.0105	0.239 0.0148	0.356 0.0222
Aluminium aileron covering	$\frac{p}{d_2}$	0.325 0.0202	0.433 0.0271	0.597 0.0376	0.841 0.0531	1.27 0.0805

The results by formula (A₁) are as follows:—

Flexural-Aileron Flutter (Fighter Aircraft)

Height (ft)	0	10,000	20,000	30,000	40,000
Fabric <i>R</i>	2.66	3.40	4.58	6.30	9.35
$\rho(R-1)$	0.00395	0.00422	0.00451	0.00472	0.00489
Aluminium <i>R</i>	8.54	11.4	15.6	22.0	33.2
$\rho(R-1)$	0.0179	0.0183	0.0184	0.0187	0.0189

The values of *K* given by equation (1) for full-scale, and based on $V_m = 800$ ft/sec and 40,000 ft, are 77 and 298 for the fabric and the aluminium covering respectively. The corresponding values, based on sea level, would be 63 and 283 respectively.

(ii) *Flexural-Aileron Flutter (Wing of R. & M. 1685²)*.—This example compares results based on formula (A₁) with damping values calculated by Falkner² for a rectangular cantilever wing ($s = 15$ ft, $c = 5$ ft). The aileron, which extended to the wing tip, was of span 7 ft and chord 1.25 ft.

Aerodynamic Coefficients ($\rho = 0.002378$)

$$\begin{array}{llll}
 b_1 = 0.334, & c_1 = 0, & e_1 = 0.0122, & f_1 = 0.211, \\
 b_2 = 0.00114, & c_2 = 0, & e_2 = 0.000517, & f_2 = 0.00302.
 \end{array}$$

The coefficients here are defined to accord with the notation of R. & M. 1685 and R. & M. 1155, and are appropriate to sea-level only.

Inertial Coefficients.—In R. & M. 1685 the standard values specified for p and d_2 are $p = 0.0011$ and $d_2 = 0.0001226$, but for the damping calculations made in that report p was increased to 0.00176, and d_2 was given the range of values $0.0001226n$, where $n = 0.2, 1.6, 5, 10, 50$.

The following table summarizes the results obtained by formula (A₁), and also gives a comparison with damping ratios read from the curves in Fig. 7 of R. & M. 1685. It should be noted that symmetrical flutter only (against a specified elastic stiffness) was assumed for the calculations in R. & M. 1685.

Flexural-Aileron Flutter (Wing of R. & M. 1685)

$p \times 10^3$	$d_2 \times 10^3$	<i>R</i> (Formula A ₁)	<i>R</i> ** (R. & M. 1685 ³)
1.1†	0.1226†	1.6	—
1.6 × standard	0.2 × standard	2.2	—
1.6 × „	1.6 × „	2.4	1.1
1.6 × „	5.0 × „	2.7	2.1
1.6 × „	10.0 × „	3.2	2.2
1.6 × „	50.0 × „	5.3	2.6

** Effective for symmetrical flutter against a specified elastic stiffness.

† 'Standard' values.

(iii) *Rudder-Torsional Flutter* (see Chap. V, R. & M. 1225⁴).—This illustration relates to a biplane on which violent rudder oscillations occurred at a flight speed of about 250 ft/sec. The principal dimensions of the tail unit were:—

Total span of tailplane 12 ft. 8 in.
 Total chord of tailplane (including elevators) .. 4 ft 8.95 in.
 Total height of rudder surface 5 ft 1.5 in.

The rudder lay wholly above the fuselage axis, and was slightly underbalanced aerodynamically by a horn.

Aerodynamic and Inertial Coefficients

Fuselage Torsional Moments		Rudder Hinge Moments	
a_1	44.7	ϕ	-1.15
b_1	1.77	b_2	0.041
c_1	0	c_2	0
ϕ	-1.15	d_2	0.745
e_1	-0.186	e_2	0.034
f_1	-0.101	f_2	0.00358

These data are taken from Table 43 of R. & M. 1255, with the gravitational cross-stiffness term omitted. The coefficients refer directly to the full-scale aircraft and to flight at sea-level. A negative product of inertia here indicates mass underbalance.

Since in the present case $\beta (\equiv b_2 f_1) < 0$, formula (A₂) must be used. The value of R works out as about 3.0, giving

$$K = 2 \times 300 \times 0.034 = 20.4$$

for $V_m = 300$ ft/sec and $\rho = 0.002378$.

3. *Numerical Examples (Class B Flutter)*.—(i) *Torsional-Aileron Flutter (Light Aircraft Wing of section 50, R. & M. 1155)*.—The basic data for this rectangular wing are given in section 5 of the Appendix to the present note, and are used there to obtain Fig. 3. The torsional axis is assumed to coincide with the flexural axis (about 0.4c behind the leading edge). The corresponding total product of inertia coefficient, deduced from inertias measured for the actual wing, is $\phi = 0.0216$ (for sea-level).

On substitution of the data, equation (2) and formula (B₁) yield $R = 2.5$. The higher root of (2) would give $R' = 7.1$, and this would ensure a test diagram of the type Fig. 2 (f). The multiplier R would, of course, normally be applied to the aileron damping.

(ii) *General Flexural-Aileron Flutter (Large Civil Transport Aircraft)*.—This example relates to a large transport aircraft ($s = 105$ ft; $c_0 = 30.35$; $l = 0.75s$). The aileron control circuit is assumed to the offset from the neutral axis of the wing, so as to provide gearing action between the flexural displacements of the wing and the angular displacements of the aileron. Owing to this gearing and the flexibility of the control circuit, a cross-stiffness is introduced in the dynamical equations for symmetrical oscillations. Elimination of this cross-stiffness by the choice of new ('barred') dynamical coordinates is accordingly necessary before formulæ (B) can be applied. The details of the treatment, which follow the lines adopted with spring tabs⁵ will be omitted, and only the essential data will be stated.

The data for the example are taken from section 11 of R. & M. 2362⁶. The derivative values are classical approximations to frequency-dependent air-load coefficients, and it should be noted that they do not accord with the simple assumption $c_1 = c_2 = 0$. A parabolic flexural mode is assumed.

Aerodynamic Coefficients (for normal control circuit).

$$\begin{array}{llll}
 b_1 = 0.7925, & c_1 = 0.3342, & e_1 = 0.000303, & f_1 = 0.3009, \\
 b_2 = 0.000866, & c_2 = 0.0004273, & e_2 = 0.000612, & f_2 = 0.002214. \\
 & \phi \text{ (aerodynamic)} = 0.00071 & & \\
 & d_2 \text{ (aerodynamic)} = 0.000019. & &
 \end{array}$$

Relations Connecting Original and Barred Coefficients.

$$\begin{aligned} \bar{b}_1 &= b_1 + N(e_1 + b_2) + N^2 e_2, & \bar{b}_2 &= b_2 + N e_2, \\ \bar{e}_1 &= e_1 + N e_2, & \bar{e}_2 &= e_2, \\ \bar{c}_1 &= c_1 + N(f_1 + c_2) + N^2 f_2, & \bar{c}_2 &= c_2 + N f_2, \\ \bar{f}_1 &= f_1 + N f_2, & \bar{f}_2 &= f_2, \\ \bar{p} &= p + N d_2, & \bar{d}_2 &= d_2, \end{aligned}$$

where N denotes the gearing ratio.

Barred Aerodynamic Coefficients (for $N = 2.5$).

$$\begin{aligned} \bar{b}_1 &= 0.799, & \bar{c}_1 &= 1.10, & \bar{e}_1 &= 0.00183, & \bar{f}_1 &= 0.306, \\ \bar{b}_2 &= 0.00240, & \bar{c}_2 &= 0.00596, & \bar{e}_2 &= 0.000612, & \bar{f}_2 &= 0.002214. \end{aligned}$$

The estimated structural inertial coefficients for sea-level were $p = 0.00210$ and $d_2 = 0.000117$, giving the following values for the total barred inertias.

Total Barred Inertial Coefficients

Height (ft)	0	10,000	20,000	30,000	40,000
\bar{p}	0.000315	0.00398	0.00525	0.00714	0.0105
\bar{d}_2	0.000136	0.000177	0.000239	0.000331	0.000494

With the present type of flexural-aileron flutter, formulæ (B), with the appropriate interchange of symbols, must of course be used, since all the aerodynamic stiffnesses are present. Moreover, the roots μ will here determine the safe bounds for the product of the *barred* direct damping coefficients. The corresponding bounds for the true direct aileron damping coefficient e_2 are then given by

$$\{b_1 + N(e_1 + b_2) + N^2 e_2\} e_2 = \mu,$$

with b_1, e_1, b_2 treated as assigned.

The final values of the minimum (true) aileron damping multipliers R , corresponding to the geared control $N = 2.5$, and to the normal control $N = 0$, are given below. The table also includes the values of the more exacting ratios R' , derived from the higher root μ_2 of equation (2) (see last footnote, Appendix).

Height (ft)	0	10,000	20,000	30,000	40,000
$N = 2.5, R$	1.5	1.9	2.4	3.3	4.8
$\rho (R-1)$	0.00119	0.00158	0.00176	0.00205	0.00223
R'	2.5	3.2	4.2	5.7	8.2
$N = 0, R$	1.6	2.0	2.7	3.6	5.3
$\rho (R-1)$	0.00143	0.00176	0.00214	0.00231	0.00252
R'	1.9	2.4	3.1	4.2	6.2

The values of the constant artificial damping, based on R and $V_m = 600$ ft/sec (about 270 m.p.h., true), are as follows.

K (lb ft/(rad/sec))

Type of Control	$h = 0$	20,000	40,000
Geared ($N = 2.5$)	960	1425	1800
Normal ($N = 0$)	1170	1730	2040

The value of V_m is here assumed to be constant for all heights.

(iii) *Servo-rudder Flutter (Aircraft X of R. & M. 1527)*.—Rudder flutter occurred on this aircraft at a speed of about 270 ft/sec. Twin rudders were fitted, symmetrically disposed about the ends of the tailplane, and a small triangular fin was present in front of each rudder. The principal rudder dimensions were as follows (see section 8, R. & M. 1527)—

Total height	165 in.
Overall chord	54.7 in.
Distance of main rudder hinge from leading edge	10.0 in.
Chord of servo-flap	10.2 in.

Calculations in connection with the binary servo-rudder flutter of this aircraft are given in sections 8 to 12 of R. & M. 1527, in section 17 of Ref. 5 and in section 3 of R. & M. 2551³. The relevant numerical data, in the notation of the last two reports, are listed below. In the present case the dynamical coefficients adopted are not non-dimensional. They correspond to the coefficients in Table 1 of the present report, with ρ , l and c_0 suppressed. All data given refer to a single rudder only.

Aerodynamic Coefficients (basic, for $\rho = 0.002378$)

Servo	$e_2 = 0.008,$	$f_2 = 0.0038,$	$j_2 = 0.025,$	$k_2 = 0.0013,$
Main Rudder	$e_3 = 0.09,$	$f_3 = 0.088,$	$j_3 = 0.80,$	$k_3 = 0.072.$

Barred Aerodynamic Coefficients ($N = 2.73, \rho = 0.002378$)

$\bar{e}_2 = 1.17,$	$\bar{f}_2 = 0.344,$	$\bar{j}_2 = 0.868,$	$\bar{k}_2 = 0.0756,$
$\bar{e}_3 = 1.045,$	$\bar{f}_3 = 0.312,$	$\bar{j}_3 = 0.80,$	$\bar{k}_3 = 0.072.$

The appropriate transformation formulae are given in section 17 of Ref. 5.

Inertias.—With the 'standard' inertial condition (leading to severe flutter on full-scale) each rudder weighed about 55 lb, and the C.G. was 12.1 in. behind the rudder hinge axis. Moreover the servo-flaps were not mass-balanced. In section 17 of Ref. 5 the critical length for a servo mass-balancing arm is given as $\lambda = 9.26$ in. The values of \bar{p} for several representative conditions are as follows :—

Standard	$\bar{p} = 6.601,$
Servo-flap statically balanced ($\lambda = 6$)	$\bar{p} = 6.912,$
Servo-flap dynamically balanced ($\lambda = 6$)	$\bar{p} = 7.047,$
Servo-flap dynamically balanced ($\lambda = 10.2$)	$\bar{p} = 6.525.$

The minimum multipliers for the true main-rudder damping are summarized below.

<i>Servo-rudder Flutter (Aircraft X)</i>		
Inertial Condition	<i>R</i> (from root μ_1)	<i>R</i> (from root μ_2)
Standard	1.33	2.43
Servo-flap statically balanced ($\lambda = 6$)	1.34	2.49
„ „ dynamically „ ($\lambda = 6$)	1.35	2.52
„ „ „ „ ($\lambda = 10.2$)	1.33	2.42

If the damping is assumed applied to the flap, instead of to the main rudder, the required minimum multiplier is of the order 13.5.

The values of artificial damping for each main rudder, derived from root μ_1 and estimated for sea-level and $V_m = 300$ ft/sec, are $K = 79$ for the standard servo and $K = 84$ for the dynamically balanced servo ($\lambda = 6$).

APPENDIX

Proofs of the Formulae

4. *Class A Binary Flutter.*—In Table 1 (a) the relevant dynamical coefficients are appropriate to flexural-aileron flutter and are expressed in the non-dimensional form. The reference section lies at a distance l from the wing root, and c_0 denotes the root chord. In this case the two dynamical coordinates are the linear normal displacement of the wing at the reference section divided by l , and the aileron angle. The inertial coefficients are expressible as follows :—

Let m denote the mass at distance y from the root and at distance $c_0\delta$ behind the aileron hinge axis. Also let f_y denote the ratio of the linear normal displacement of the wing at distance y from the root to the corresponding displacement at the reference section. Then the total inertial coefficients are given by

$$a_1 = \left(\sum_w m f_y^2 / \rho l c_0^2 \right) + a_{10},$$

$$p = \left(\sum_a m \delta f_y / \rho l c_0^2 \right) + p_0,$$

$$d_2 = \left(\sum_a m \delta^2 / \rho l c_0^2 \right) + d_{20},$$

where a_{10} , p_0 , d_{20} denote the aerodynamic inertias, and \sum_w , \sum_a denote respectively summation over the complete wing (with aileron) and over the aileron only.

Fig. 1 (a) shows the normal type of test-conic diagram for flexural-aileron flutter, when the aileron is mass-underbalanced. The stiffness point $Z(0, f_2)$ has the positive ordinate f_2 , and the points of intersection M, N, M', N' of the conic with the coordinate axes are all real. In particular, the positions of M and N are given by $OM = \beta/b_1$ and $ON = \beta/e_2$. Hence

$$OZ - OM = |bf|/b_1.$$

The first essential condition for absolute prevention of flutter is that Z shall be above M : this requires

$$|bf| > 0.$$

This inequality cannot, of course, be controlled by changes of the direct aileron damping e_2 , and must be assumed to be already satisfied. If in fact Z lies below M , the minimum aileron damping indicated by the present theory should ensure high critical speeds and will almost certainly be as effective as mass-balancing.

Two cases arise, according as $\beta > 0$ or < 0 .

Case (i) ($\beta > 0$).—This is representative of standard flexural-aileron flutter, and corresponds to OM and ON, both positive.

Let MM_1 in Fig. 1 (a) be the chord parallel to OX. Then it is readily shown that M_1 lies to the right, or to the left, of M according as

$$W \equiv b_1^2 e_2^2 - b_1 e_2 (b_2 e_1 + p f_1) + b_2 f_1 \{p (e_1 + b_2) - d_2 b_1\} < 0 \text{ or } > 0.$$

Hence if e_2 is regarded as variable and is chosen so great that $W > 0$, the conic is necessarily disposed as in Fig. 1 (b), and flutter is prevented absolutely. The minimum safe value of e_2 is given by the greatest root of the equation $W = 0$; M_2 and M then coincide, and OM is the maximum ordinate (see Fig. 1 (c)).

If the equation $W = 0$ (which corresponds to formula (A₂) of the main text) has unreal roots, W is necessarily positive. Increased damping is then not required.

Case (ii) ($\beta < 0$).—This case arises with rudder fuselage-torsional flutter. If the fuselage torsional moments and the rudder hinge moments are taken to correspond respectively to the left-hand and right-hand entries in Table 1 (a), the signs of e_1 and f_1 will be negative and the remaining coefficients will be positive. Then Z lies above O, but OM and ON are both negative, since $\beta < 0$. In this case the condition $W > 0$ (i.e. M_1 to left of M) does not preclude flutter, as shown by Fig. 1 (d). However, a relatively simple sufficient condition is given by the restriction that M' shall not lie above O. This ensures a safe test diagram of the type Fig. 1 (e). The minimum value of e_2 is here given by the greatest root of the quadratic equation

$$\{a_1 e_2 + b_1 d_2 - p (e_1 + b_2)\} \{b_1 e_2 - b_2 e_1 - p (e_1 + b_2)\} + (a_1 d_2 - p^2) b_2 f_1 = 0.$$

This corresponds to formula (A₂) of the main text. A more exacting, but simpler, sufficient condition is that M' shall not lie above M . This would give the damping value*

$$b_1 e_2 = b_2 e_1 + p f_1 - \frac{a_1 b_2 f_1}{b_1}.$$

Summary.—Let e_2 , Re_2 denote respectively the natural direct damping coefficient, and the minimum coefficient accepted for safety. Then the formulae are

Case (i) ($f_2 > 0$, $\beta > 0$).

$$b_1^2 e_2^2 R^2 - b_1 e_2 (b_2 e_1 + p f_1) R + b_2 f_1 \{p (e_1 + b_2) - d_1 b_2\} = 0. \quad \dots \quad (A_1)$$

Case (ii) ($f_2 > 0$, $\beta < 0$).

$$\{a_1 e_2 R + b_1 d_2 - p (e_1 + b_2)\} \{b_1 e_2 R - b_2 e_1 - p (e_1 + b_2)\} + (a_1 d_2 - p^2) b_2 f_1 = 0. \quad (A_2)$$

In each case the greatest root is to be taken.

* See Equation (129) of R. & M. 1155¹.

5. *Class B, Binary Flutter.*—Table 1 (b) defines the dynamical coefficients. With torsional-aileron flutter the dynamical coordinates would be the wing twist at the reference section, and the aileron angle at the reference section. The inertias would then be defined as follows.

Let m denote the mass at distance y from the wing root and at distance $c_0\delta$ behind the aileron hinge axis. Also let this axis* lie at distance c_0D behind the axis of twist OY. Then, if F_y denotes the ratio of the twist at section y † to that at the reference section, the total inertial coefficients required are

$$d_2 = \left(\sum_a m\delta^2/\rho l c_0^2 \right) + d_{20},$$

$$p = \left(\sum_a m\delta (\delta + DF_y)/\rho l c_0^2 \right) + p_0.$$

Fig. 2 (a) shows the normal type of test conic diagram for torsional-aileron flutter. The stiffness point Z lies at (k_2, f_3) , and the points M, N which are common to the test conic T, the frequency line LL, and the upper branch H_u , of the divergence hyperbola, are given by‡

$$2j_3X_M = \beta - \Omega, \quad 2e_2Y_M = \beta + \Omega,$$

$$2j_3X_N = \beta + \Omega, \quad 2e_2Y_N = \beta - \Omega,$$

where

$$\Omega^2 \equiv \beta^2 - 4\mu k_2 f_3,$$

$$\beta \equiv j_2 f_3 + e_3 k_2,$$

$$\mu \equiv e_2 j_3 \text{ (product of direct damping coefficients).}$$

The points M, N are accordingly unreal when μ exceeds the critical value (Fig. 2 (b))

$$\mu = \beta^2/4k_2 f_3.$$

The conic T then lies either wholly below H_u , or wholly above (cases of Fig. 2 (c)). In the first case flutter is either prevented absolutely or cannot occur before divergence. In the second case it is possible by further increases of μ first to shrink the test conic to a point (Fig. 2 (d)), and then make it unreal (Fig. 2 (e)). If μ is increased sufficiently, the ellipse again becomes real (Fig. 2 (f)), but is situated below H_u . To determine the limiting values of μ certain further formulae are required.

First, the condition for an imaginary test conic is§

$$f \equiv \mu^2 - 2\mu p (k_2 + f_3) + p^2 (k_2 - f_3)^2 - \mu e_3 j_2 + p\beta (j_2 + e_3) < 0. \quad (3)$$

Again, when the conic is real but M, N are unreal, the ellipse will lie below or above H_u (Fig. 2 (c)) according as the pole Q of the frequency line LL with respect to the conic lies below or above LL. The co-ordinates of Q are found to be

$$\frac{X_Q}{d_2\Omega^2 + e_2R} = \frac{Y_Q}{g_3\Omega^2 + j_3R} = \frac{1}{2\mu\alpha + p\beta (j_2 + e_3)},$$

where

$$R \equiv |ej| \beta + p\beta' (k_2 - f_3).$$

* For simplicity the hinge axis is here assumed to be parallel to OY.

† See for example, section 7 of Ref. 5.

‡ See section (c) of R. & M. 1155¹.

§ See Equation (72) of R. & M. 1155¹.

These relations yield, after some reduction

$$j_3 X_Q + e_2 Y_Q - \beta = \frac{\Omega^2 q_1'}{2\mu\alpha + p\beta(j_2 + e_3)}.$$

Hence, if attention is restricted to the case $\Omega^2 < 0$ (M, N unreal) the point Q lies below or above H_u according as

$$2\mu\alpha + p\beta(j_2 + e_3) > 0 \text{ or } < 0.$$

On substitution for α from Table 1 this inequality can be written

$$g \equiv 2\mu^2 - 2\mu p(k_2 + f_3) - 2\mu e_3 j_2 + p\beta(j_2 + e_3) > 0 \text{ or } < 0. \quad \dots \quad (4)$$

The inequalities (3) and (4) are most simply discussed by a graphical representation of the two conics $f = 0$, $g = 0$, in the (μ, p) plane (Fig. 3). Both conics are hyperbolic, and their main characteristics are as follows.

Hyperbola $f = 0$.

(i) *Intercepts on axes*

$$\begin{aligned} p = 0, \quad \mu = 0 \text{ and } \mu = e_3 j_2, \\ \mu = 0, \quad p = -\frac{\beta(j_2 + e_3)}{(k_2 - f_3)^2}. \end{aligned}$$

(ii) *Centre*

$$\begin{aligned} 8k_2 f_3 \mu &= \beta^2 + k_2 f_3 (j_2 + e_3)^2, \\ 8k_2 f_3 p &= j_2^2 f_3 + e_3^2 k_2. \end{aligned}$$

(iii) *Asymptotes.*

$$\begin{aligned} \mu - p(k_2 + f_3 + 2\sqrt{k_2 f_3}) &= -\frac{(j_2 \sqrt{f_3} - e_3 \sqrt{k_2})^2}{4\sqrt{k_2 f_3}}, \\ \mu - p(k_2 + f_3 - 2\sqrt{k_2 f_3}) &= \frac{(j_2 \sqrt{f_3} + e_3 \sqrt{k_2})^2}{4\sqrt{k_2 f_3}}. \end{aligned}$$

Hyperbola $g = 0$.

(i) *Intercepts on axes*

$$p = 0, \quad \mu = 0 \text{ and } \mu = e_3 j_2.$$

(ii) *Centre.*

$$\begin{aligned} 2(k_2 + f_3)\mu &= \beta(j_2 + e_3), \\ (k_2 + f_3)^2 p &= j_2^2 f_3 + e_3^2 k_2. \end{aligned}$$

(iii) *Asymptotes*

$$\mu = \frac{\beta(j_2 + e_3)}{2(k_2 + f_3)},$$

$$\mu - p(k_2 + f_3) + \frac{\beta'(j_2 - e_3)}{2(k_2 + f_3)} = 0.$$

The four points of intersection of the two curves are given by (Fig. 3)

$$\begin{aligned} \mu &= 0, & \phi &= 0 \text{ (origin O)}, \\ \mu &= e_3 j_2, & \phi &= 0 \text{ (point S)}, \\ 4\mu &= (j_2 + e_3)^2, & 4\phi (k_2 - f_3) &= j_2^2 - e_3^2 \text{ (point K)}, \\ 4k_2 f_3 \mu &= \beta^2, & 4k_2 f_3 (k_2 - f_3) \phi &= -\beta \beta' \text{ (point J)}. \end{aligned}$$

The tangents to $f = 0$ at K and J are parallel to $\mu = 0$, and are

$$\begin{aligned} \mu &= (j_2 + e_3)^2/4 \text{ (tangent AA' at point K)}, \\ \mu &= \beta^2/4k_2 f_3 \text{ (tangent BB' at point J)}. \end{aligned}$$

The region of the (μ, ϕ) diagram to the right of AA' corresponds to $\Delta \equiv 4\mu - (j_2 + e_3)^2 > 0$ and so to elliptic test conics. The region to the right of BB' corresponds to the cases where M, N are unreal ($\Omega^2 < 0$).

Fig. 3 is the diagram appropriate to torsional-aileron flutter of the rectangular light aircraft wing ($s = 9$ ft, $c_0 = 3$ ft) specified in section 50 of R. & M. 1155¹. The torsional axis is assumed to be coincident with the flexural axis (14.5 in from leading edge). As in R. & M. 1155¹ the reference section is chosen at the wing tip ($l = s$), and the appropriate derivative coefficients (converted from Table 16 of R. & M. 1155 to accord with the definitions in Table 1 of the present report) are

$$\begin{aligned} e_2 &= 0.0046, & e_3 &= 0.020, \\ f_2 &= 0.0090, & f_3 &= 0.045, \\ j_2 &= 0.0087, & j_3 &= 0.054, \\ k_2 &= 0.0048, & k_3 &= -0.080. \end{aligned}$$

The value of the natural main damping product is $\mu \equiv e_2 j_2 = 2.484 \times 10^{-4}$.

These data yield

Point S	$10^{-4} (1.74, 0)$
Point K	$10^{-4} (2.06, 20.17)$
Point J	$10^{-4} (2.75, 41.5)$
Centre of $f = 0$	$10^{-4} (2.4, 30.4)$
Centre of $g = 0$	$10^{-4} (1.4, 21.5)$
Asymptotes of $f = 0$	$\mu - 0.792\phi = -3.58 \times 10^{-6}$
	$\mu - 0.020\phi = 1.77 \times 10^{-4}$
Asymptotes of $g = 0$	$\mu = 1.4 \times 10^{-4}$
	$\mu - 0.05\phi = 0.34 \times 10^{-4}$.

Points on the upper hyperbolic branch VJW of $f = 0$ indicate reduction of the test conic T to a point. This degenerate ellipse lies below or above H_u (Figs. 2 (f)) and 2 (d)) according as the lower segment JV, or the upper segment JW, is taken. Hence, the safe region of the (μ, ϕ) diagram lies to the right of the composite boundary* BJW.

Summary.—Let μ_1, μ_2 denote the two roots of the equation

$$\mu^2 - \mu \{e_3 j_2 + 2\phi (k_2 + f_3)\} + \phi^2 (k_2 - f_3)^2 + \phi \beta (j_2 + e_3) = 0.$$

Then if μ_1, μ_2 are real ($\mu_2 > \mu_1$) the multiplier R to be applied to the product $e_2 j_3$ is given by

$$R = \mu_1 / e_2 j_3. \quad \dots \dots \dots (B_1)$$

If μ_1, μ_2 are unreal

$$R = \beta^2 / 4e_2 j_3 k_2 f_3. \quad \dots \dots \dots (B_2)$$

* A limitation to the region to the right of BJW would be unnecessarily severe, and would correspond to the values R' quoted in some of the numerical examples.

REFERENCES

No.	Author	Title, etc.
1	R. A. Frazer and W. J. Duncan..	The Flutter of Aeroplane Wings. R. & M. 1155. August, 1928.
2	V. M. Falkner	Effect of Variation of Aileron Inertia and Damping on Flexural-aileron Flutter of a Typical Cantilever Wing. R. & M. 1685. October, 1935.
3	R. A. Frazer	Graphical Treatment of Binary Mass-balancing Problems. R. & M. 2551. August, 1942.
4	R. A. Frazer and W. J. Duncan..	The Flutter of Monoplanes, Biplanes and Tail Units. R. & M. 1225. May, 1927.
5	R. A. Frazer and W. P. Jones ..	Wing-aileron-tab Flutter. A.R.C. 5668. March, 1942. (To be published).
6	W. P. Jones	Effect of a Flexurally-gearred Aileron Control on the Binary Flutter of a Wing-aileron System. R. & M. 2362. February, 1924.
7	W. J. Duncan and A. R. Collar ..	Binary Servo-rudder Flutter. R. & M. 1527. February, 1933.

TABLE 1
Dynamical Coefficients and Supplementary Symbols
 (a) Class A Flutter (Typified by Flexural-Aileron Flutter).

Flexural Moments			Aileron hinge-Moments		
Coefficient	Significance	Non-dimensional Form	Coefficient	Significance	Non-dimensional Form
A_1	Inertia	$\rho l^3 c_0^2 a_1$	P	Inertia	$\rho l^2 c_0^3 p$
B_1	$-L_\phi$	$\rho V l^3 c_0 b_1$	B_2	$-H_\phi$	$\rho V l^2 c_0^2 b_2$
C_1	l_ϕ	$\rho V^2 l^3 X$	0		0
P	Inertia	$\rho l^2 c_0^3 p$	D_2	Inertia	$\rho l c_0^4 d_2$
E_1	$-L_\xi$	$\rho V l^2 c_0^2 e_1$	E_2	$-H_\xi$	$\rho V l c_0^3 e_2$
F_1	$-L_\xi$	$\rho V^2 l^2 c_0 f_1$	F_2	$h_\xi - H_\xi$	$\rho V^2 l c_0^2 Y$

$$\begin{aligned}
 X &\equiv l_\phi / \rho V^2 l^3, & Y &\equiv (h_\xi / \rho V^2 l c_0^2) + f_2, \\
 |be| &\equiv b_1 e_2 - b_2 e_1, & |bf| &\equiv b_1 f_2 - b_2 f_1, \\
 \alpha &\equiv |be| - pf_1, & \beta &\equiv b_2 f_1, \\
 q_1' &\equiv a_1 e_2 + b_1 d_2 - p(e_1 + b_2), & \Delta &\equiv 4b_1 e_2 - (e_1 + b_2)^2.
 \end{aligned}$$

(b) Class B Flutter (Typified by Torsional-aileron Flutter)

Aileron hinge-Moments			Wing Torsional Moments		
Coefficient	Significance	Non-dimensional Form	Coefficient	Significance	Non-dimensional Form
D_2	Inertia	$\rho l c_0^4 d_2$	P	Inertia	$\rho l c_0^4 p$
E_2	$-H_\xi$	$\rho V l c_0^3 e_2$	E_3	$-M_\xi$	$\rho V l c_0^3 e_3$
F_2	$h_\xi - H_\xi$	$\rho V^2 l c_0^2 X$	F_3	$-M_\xi$	$\rho V^2 l c_0^2 f_3$
P	Inertia	$\rho l c_0^4 p$	G_3	Inertia	$\rho l c_0^4 g_3$
J_2	$-H_\theta$	$\rho V l c_0^3 j_2$	J_3	$-M_\theta$	$\rho V l c_0^3 j_3$
K_2	$-H_\theta$	$\rho V^2 l c_0^2 k_2$	K_3	$m_\theta - M_\theta$	$\rho V^2 l c_0^2 Y$

$$\begin{aligned}
 X &\equiv (h_\xi / \rho V^2 l c_0^2) + f_2, & Y &\equiv (m_\theta / \rho V^2 l c_0^2) + k_3, \\
 \beta &\equiv j_2 f_3 + e_3 k_2, & \alpha &\equiv |ej| - p(k_2 + f_3), \\
 \beta' &\equiv j_2 f_3 - e_3 k_2, & \Omega &\equiv + \sqrt{\beta^2 - 4e_2 j_3 k_2 f_3}, \\
 q_1' &\equiv d_2 j_3 + g_3 e_1 - P(j_1 + e_2), & \Delta &\equiv 4e_2 j_3 - (j_2 + e_3)^2.
 \end{aligned}$$

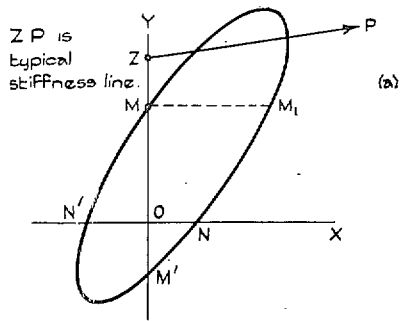
TABLE 2

Summary of Results of Numerical Examples (sections 2 and 3)

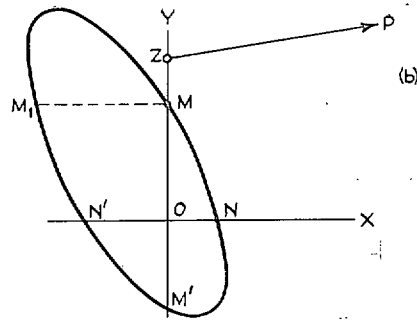
Aircraft Type	V_m (ft/sec)	Flutter Type	Specification of Control Surface	Multiplier R (main control surface)			Artificial Damping K (lb ft/rad/sec)		
				$h = 0$	20,000	40,000	$h = 0$	20,000	40,000
Modern fighter ^{3, 5} (example 2 (i))	800	Flexural-aileron	Fabric covered ailerons ..	2.7	—	9.4	63	—	77
			Aluminium covered ..	8.5	—	33	283	—	298
Biplane (example 2 (iii)) ..	300	Rudder-torsional	Rudder horn-balanced and above fuselage axis	3.0	—	—	20.4	—	—
Large civil transport ⁶ (example 3(ii))	600	Flexural - aileron (geared)	Control circuit offset from neutral axis	1.5	2.4	4.8	960	1425	1800
		Flexural - aileron	Control circuit normal ..	1.6	2.7	5.3	1170	1730	2040
Military transport ⁷ (twin-tail) (example 3 (iii)).	300	Servo-rudder ..	Servo not mass-balanced	1.33	—	—	79	—	—
			Servo dynamically balanced	1.35	—	—	84	—	—

Notes. (a) R is defined as the ratio of the minimum direct damping coefficient for absolute flutter prevention to the natural direct damping coefficient.

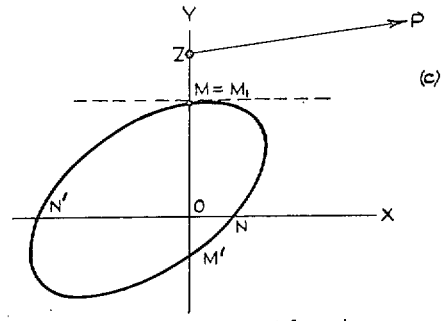
(b) K denotes the constant artificial damping to be applied to each relevant main control surface, and measures the additional damping hinge moment (lb ft) when that surface is turned uniformly at the rate of 1 rad/sec.



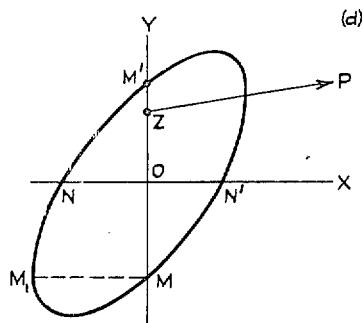
Flexure - Aileron Flutter ($\beta > 0$)
Normal Aileron Damping e_2 .



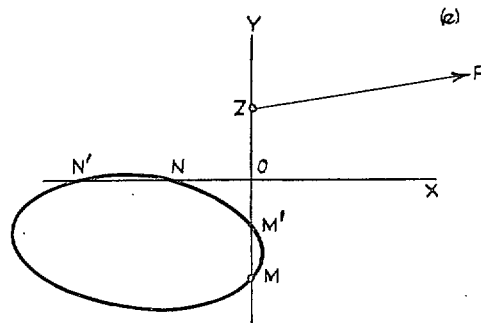
Flexure - Aileron Flutter ($\beta > 0$)
Flutter Prevented ($W > 0$).



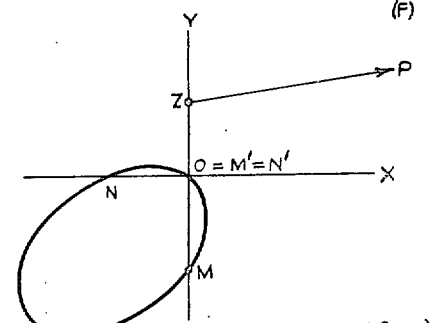
Flexure - Aileron Flutter ($\beta > 0$)
Flutter Prevented ($W=0$, Formula A₁).



Rudder - Torsion Flutter ($\beta < 0$)
Flutter Present ($W > 0$)

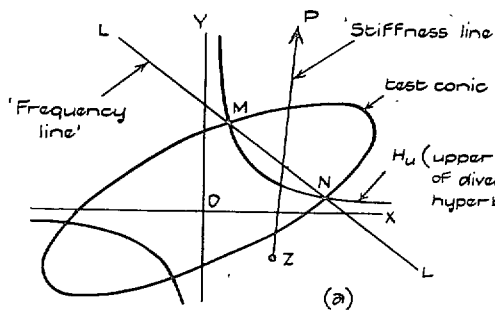


Rudder - Torsion Flutter ($\beta < 0$)
Flutter Prevented (M' below O)

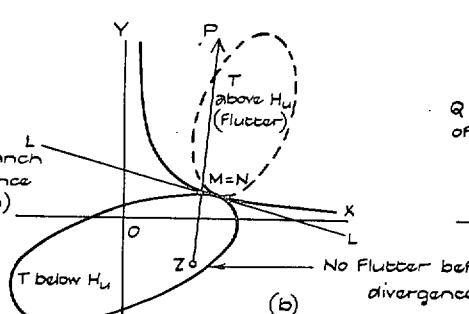


Rudder - Torsion Flutter ($\beta < 0$)
Flutter Prevented (Formula A₂).

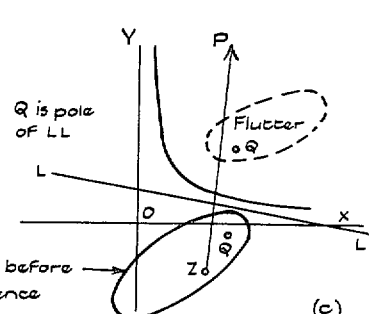
FIG. 1. Test Conics for Class A Flutter.



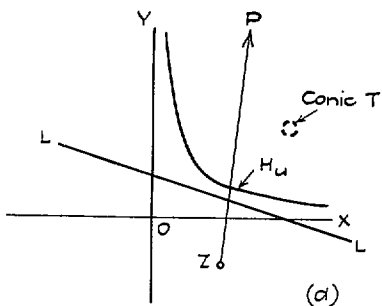
Normal Damping Product ($\mu = e_2 j_3$)



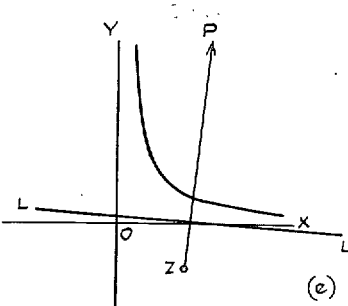
The Two Cases of Contact ($\mu = \beta^2 / 4k_2 f_3$)



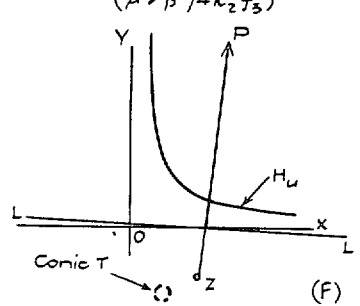
Cases M, N unreal ($\mu > \beta^2 / 4k_2 f_3$)



Test Conic a Point Ellipse above H_u
($\mu = \mu_1$; Formula B₁)



Test Conic Unreal
($\mu_2 > \mu_1$; no Flutter)



Test Conic a Point Ellipse
below H_u ($\mu = \mu_2$)

FIG. 2. Test Conics for Class B Flutter.

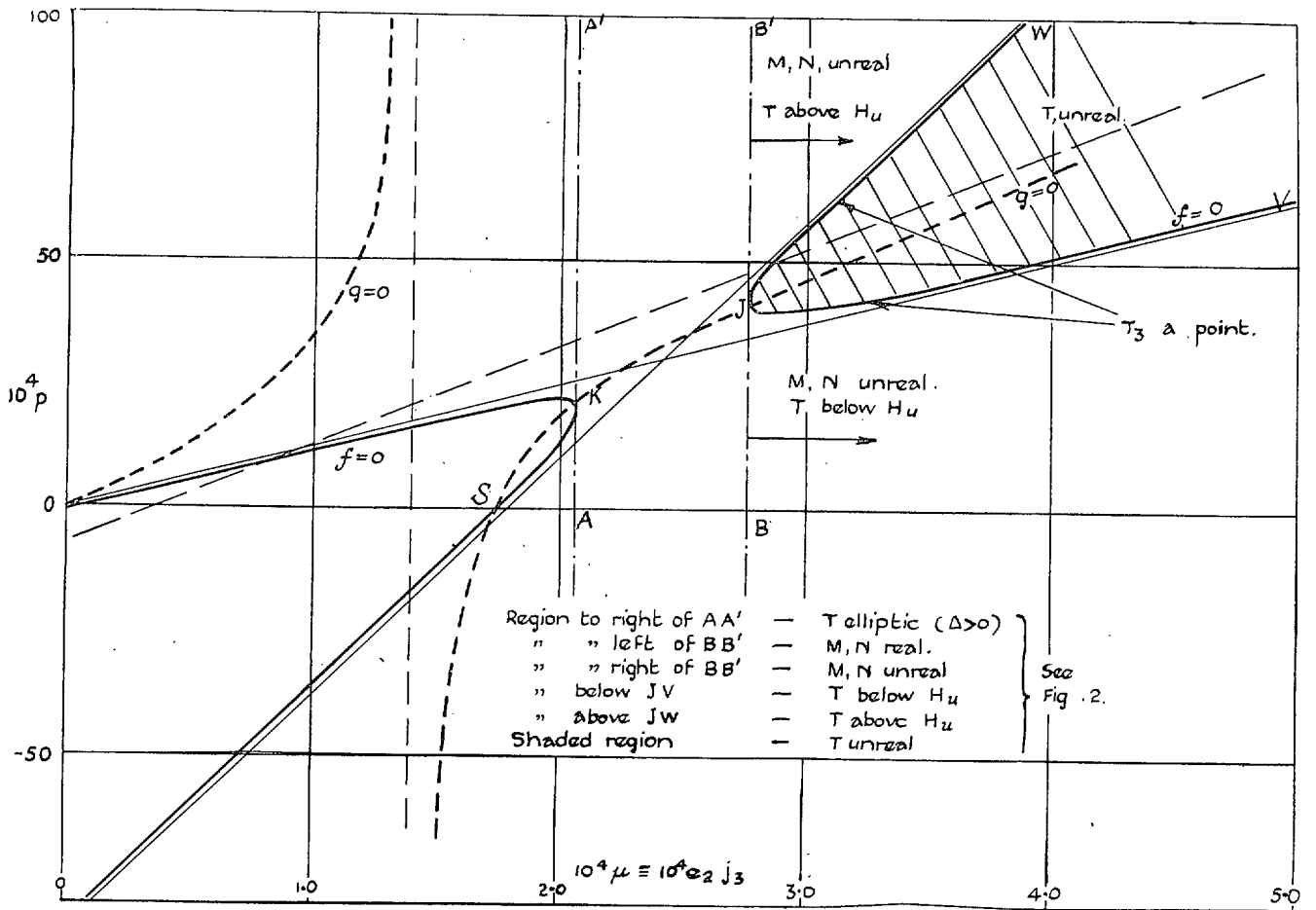


FIG. 3. Illustrative (μ, p) Diagram (see Section 5).

Publications of the Aeronautical Research Council

ANNUAL TECHNICAL REPORTS OF THE AERONAUTICAL RESEARCH COUNCIL (BOUND VOLUMES)—

- 1934-35 Vol. I. Aerodynamics. *Out of print.*
Vol. II. Seaplanes, Structures, Engines, Materials, etc. 40s. (40s. 8d.)
- 1935-36 Vol. I. Aerodynamics. 30s. (30s. 7d.)
Vol. II. Structures, Flutter, Engines, Seaplanes, etc. 30s. (30s. 7d.)
- 1936 Vol. I. Aerodynamics General, Performance, Airscrews, Flutter and Spinning.
40s. (40s. 9d.)
Vol. II. Stability and Control, Structures, Seaplanes, Engines, etc. 50s. (50s. 10d.)
- 1937 Vol. I. Aerodynamics General, Performance, Airscrews, Flutter and Spinning.
40s. (40s. 10d.)
Vol. II. Stability and Control, Structures, Seaplanes, Engines, etc. 60s. (61s.)
- 1938 Vol. I. Aerodynamics General, Performance, Airscrews. 50s. (51s.)
Vol. II. Stability and Control, Flutter, Structures, Seaplanes, Wind Tunnels,
Materials. 30s. (30s. 9d.)
- 1939 Vol. I. Aerodynamics General, Performance, Airscrews, Engines. 50s. (50s. 11d.)
Vol. II. Stability and Control, Flutter and Vibration, Instruments, Structures,
Seaplanes, etc. 63s. (64s. 2d.)
- 1940 Aero and Hydrodynamics, Aerofoils, Airscrews, Engines, Flutter, Icing, Stability
and Control, Structures, and a miscellaneous section. 50s. (51s.)

*Certain other reports proper to the 1940 volume will subsequently be
included in a separate volume.*

ANNUAL REPORTS OF THE AERONAUTICAL RESEARCH COUNCIL—

1933-34	1s. 6d. (1s. 8d.)
1934-35	1s. 6d. (1s. 8d.)
April 1, 1935 to December 31, 1936.	4s. (4s. 4d.)
1937	2s. (2s. 2d.)
1938	1s. 6d. (1s. 8d.)
1939-48	3s. (3s. 2d.)

INDEX TO ALL REPORTS AND MEMORANDA PUBLISHED IN THE ANNUAL TECHNICAL REPORTS, AND SEPARATELY—

April, 1950 R. & M. No. 2600. 2s. 6d. (2s. 7½d.)

INDEXES TO THE TECHNICAL REPORTS OF THE AERONAUTICAL RESEARCH COUNCIL—

December 1, 1936 — June 30, 1939.	R. & M. No. 1850. 1s. 3d. (1s. 4½d.)
July 1, 1939 — June 30, 1945.	R. & M. No. 1950. 1s. (1s. 1½d.)
July 1, 1945 — June 30, 1946.	R. & M. No. 2050. 1s. (1s. 1½d.)
July 1, 1946 — December 31, 1946.	R. & M. No. 2150. 1s. 3d. (1s. 4½d.)
January 1, 1947 — June 30, 1947.	R. & M. No. 2250. 1s. 3d. (1s. 4½d.)

Prices in brackets include postage.

Obtainable from

HIS MAJESTY'S STATIONERY OFFICE

York House, Kingsway, LONDON, W.C.2 429 Oxford Street, LONDON, W.1
P.O. Box 569, LONDON, S.E.1

13a Castle Street, EDINBURGH, 2 1 St. Andrew's Crescent, CARDIFF
39 King Street, MANCHESTER, 2 Tower Lane, BRISTOL, 1
2 Edmund Street, BIRMINGHAM, 3 80 Chichester Street, BELFAST

or through any bookseller.